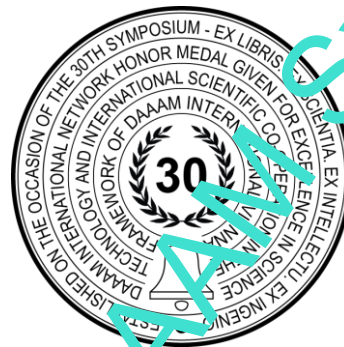


ANALYSIS OF CLAMPING OPTIMIZATION FOR HFM CONNECTOR DURING MEASUREMENT

Nikola Skřivanová, Martin Melichar & Kateřina Kašová



This Publication has to be referred as: Skřivanova, N[ikola]; Melichar, M[artin] & Kasova, K[aterina] (2022). Analysis of clamping optimization for HFM connector during measurement. Proceedings of the 33rd DAAAM International Symposium, pp.xxxx-xxxx, B. Katalinic (Ed.), Published by DAAAM International, ISBN 978-3-902734-xx-x, ISSN 1726-9679, Vienna, Austria
DOI: 10.2507/33rd.daaam.proceedings.xxx

Abstract

This paper focuses on the quantification of the influence and optimization of HFM connector clamping in the evaluation of the concentricity of internal contact against the external rosette in the automotive industry. It is related to the article Analysis of clamping effect in HFM connector measurement. In the previous experiment, which was carried out in an accredited laboratory of an automotive company, the negative effect of HFM connector clamping in concentricity measurements using a Keyence VHX-5000 digital microscope was found. Now the previous findings have been verified and a new way of clamping the parts has been devised. The new clamping method eliminated this negative effect. This benefit is best demonstrated by the data obtained.

Keywords: uncertainty of measurement; clamping; CMM; digital microscope

1. Introduction

This article is a follow-up to the article Analysis of the effect of clamping in HFM connector measurements, in which the effect of negative clamping of the HFM connector in concentricity measurements using the Keyence VHX-5000 digital microscope was determined. Thus, the problem and its cause were found in the previous experiment. Subsequently, the question arose, how to achieve optimal clamping without a negative contribution to the measurement result? Therefore, the next experiment consisted in verifying the consistency of the measurement using the EN parameter and quantifying the new clamping. With the new type of clamping, this effect was eliminated. This result is represented by the obtained measurement data and verified by calculations. Thus, we can conclude that the problem that the accredited laboratory had been solved.

2. Determination of measurement uncertainty for Keyence VHX-5000

The part was repeatedly clamped at each measurement. From these measurements, the uncertainty of the type A measurement was calculated. Other uncertainty components were determined: temperature variation and MPE of the measuring device. The input data and calculations are presented in the following tables. Since this equipment can be

operated by more than one laboratory personnel, two personnel were selected to make the specified measurements independently and the uncertainty was then calculated for each of them so that they could be compared with each other.

Measured parameter - concentricity - tolerance	0,23mm
MPE (2,6+L/170) μm	0,0038mm
Temperature in the laboratory	23°C
Temperature fluctuations	2°
Coefficient of thermal expansion α spring bronze	0,000018mm

Table 1. Input data

Systematic error at 23°C	$\Delta L_{20^{\circ}C} = \alpha \cdot \Delta T$	L=0,000018*3	0,000054mm
Fluctuation 2°C	$\Delta L_{kol.} = \alpha \cdot \Delta T$	L=0,000018*2	0,000036mm

Table 2. Calculation of the effect of temperature change

1	2	3	4	5	6	7	8	9	10
0,126m	0,108m	0,116m	0,102m	0,118m	0,110m	0,105m	0,120m	0,106m	0,114m
m	m	m	m	m	m	m	m	m	m

Table 3. Measured values (10 repetitions) - worker A

1	2	3	4	5	6	7	8	9	10
0,142m	0,112m	0,102m	0,134m	0,116m	0,130m	0,124m	0,128m	0,142m	0,104m
m	m	m	m	m	m	m	m	m	m

Table 4. Measured value (10 repetitions) - worker B

Average of measured values	=PRŮMĚR()	0,113mm
Selection directional deviation	=SMODCH.VÝBĚR.S()	0,0074863mm
Average correction to 20°C	$\bar{X} \text{ korigovaný} = \bar{X} - L_{20^{\circ}C}$	0,113mm
u_A	$u_A = k_{UA} \cdot \frac{s}{\sqrt{n}}$	0,00237mm

Table 5. Calculation of Type A measurement uncertainty based on repeated measurements - Worker A [7], [8]

Average of measured values	=PRŮMĚR()	0,123mm
Selection directional deviation	=SMODCH.VÝBĚR.S()	0,0144852mm
Average correction to 20°C	$\bar{X} \text{ korigovaný} = \bar{X} - L_{20^{\circ}C}$	0,123mm
u_A	$u_A = k_{UA} \cdot \frac{s}{\sqrt{n}}$	0,00458mm

Table 6. Calculation of Type A measurement uncertainty based on repeated measurements - Worker B [7], [8]

	Zmax	χ	u_{bi}	u_{bi}
MPE Keyence VHX	0,0038mm	1,732051	$u_{bi} = \frac{Zmax}{\chi}$	0,002193931
Temperature fluctuation 2°C	0,00000828mm	1,732051	$u_{bi} = \frac{Zmax}{\chi}$	0,000000478
Calculation of the standard combined uncertainty				
u_y	=ODMOCNINA(SUMA.ČTVERCŮ($u_A; u_{bivertex}; u_{bikol}$))			0,003227662
Calculation of the expanded combined uncertainty				
U	=2 · u_y			0,007mm

Table 7. Calculation of type B measurement uncertainty and expanded combined uncertainty U - worker A [7], [8]

	Zmax	χ	u_{bi}	u_{bi}
MPE Keyence VHX	0,0038mm	1,732051	$u_{bi} = \frac{Zmax}{\chi}$	0,002193931
Temperature fluctuation 2°C	0,00000828mm	1,732051	$u_{bi} = \frac{Zmax}{\chi}$	0,000000478
Calculation of the standard combined uncertainty				
u_y	=ODMOCNINA(SUMA.ČTVERCŮ($u_A; u_{bivertex}; u_{bikol}$))			0,005078935
Calculation of the expanded combined uncertainty				
U	=2 · u_y			0,011mm

Table 8. Calculation of type B measurement uncertainty and expanded combined uncertainty U - worker B [7], [8]

The measurement result of operator A with the specified expanded combined uncertainty =0.113mm +/- 0.007mm. The measurement result of operator B with the specified expanded combined uncertainty is 0.123mm +/- 0.011mm.

5. Assessment of the measurement results of operators A and B

At first glance, the difference in the measurement results of the Keyence VHX-5000 obtained when changing the operator is noticeable. The result obtained with operator A is 0.113 mm +/- 0.007 mm. The result obtained with operator B is 0.123 mm +/- 0.011 mm. The EN parameter can be used to assess the agreement between the results of the two operators under the condition that $EN \leq 1$.

$$E_n = \frac{\bar{x}_{lab} - \bar{x}_{pilot}}{\sqrt{U_{lab}^2 + U_{pilot}^2}} \quad |E_n| \leq 1,$$

\bar{x}_{lab} = the average of the measured values of the operator, in our case operator B,

\bar{x}_{pilot} = the average of the measured values of the operator - pilot, in our case operator A,

U_{lab} = the extended combined uncertainty of the operator, in our case operator B,

U_{pilot} = the extended combined uncertainty of the operator, in our case operator A.

After substituting the values into the formula, we obtain the value $EN = 0.77$. This value satisfies the condition $|EN| \leq 1$. Based on the EN calculation, the resulting value is within tolerance, although it is close to the warning value of 0.80.

When comparing the sampling standard deviations and calculated uncertainties of the type A measurements between operator A and operator B, it is clear that not all random effects entering the measurement system have been sufficiently removed. The resulting values are:

the sampling standard deviation of operator A = 0,0074863mm,

the sampling standard deviation of operator B = 0,0144852mm,

u_A operator A = 0,00237mm,

u_A operator B = 0,00458mm.

Analysis of the measuring system due to differences between operators A and B revealed a significant contribution of unstable part clamping, which increases the measurement uncertainty. This contribution was reduced by constructing a more suitable and stable part clamping under the microscope objective.

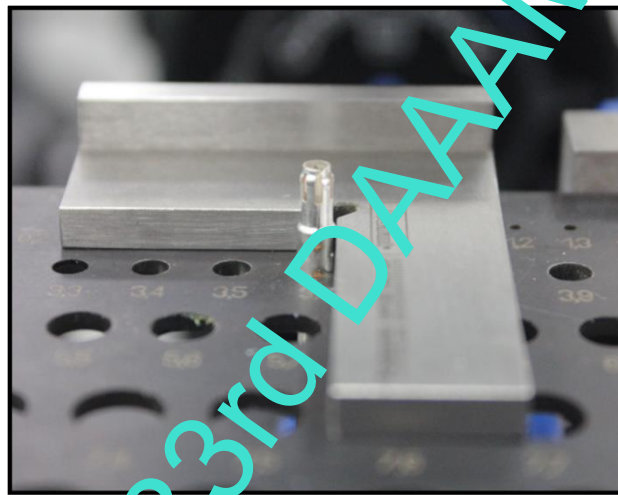


Table 9. More stable clamping of the HFM connector

6. Recalculation of the measurement uncertainty after clamping optimization in the measurement system

After setting up the new clamping system and sensitizing the operator, the whole procedure of determining the measurement uncertainties was repeated. The repeat measurement was performed under the same input conditions with the same operators A and B as in section 4.2.

1	2	3	4	5	6	7	8	9	10
0,115m	0,111m	0,114m	0,118m	0,108m	0,111m	0,120m	0,109m	0,113m	0,111m
m	m	m	m	m	m	m	m	m	m

Table 10. Measured values (10 repetitions) - worker A [7], [8]

1	2	3	4	5	6	7	8	9	10
0,124m	0,108m	0,116m	0,104m	0,126m	0,114m	0,126m	0,122m	0,106m	0,106m
m	m	m	m	m	m	m	m	m	m

Table 11. Measured values (10 repetitions) - worker B [7], [8]

Average of measured values	=PRŮMĚR()	0,113mm
Selection directional deviation	=SMODCH.VÝBĚR.S()	0,0039001mm
Average correction to 20°C	$\bar{X} \text{ korigovaný} = \bar{X} - L_{20^\circ C}$	0,113mm
u_A	$u_A = k_{UA} \cdot \frac{S}{\sqrt{n}}$	0,0022mm

Table 12. Calculation of Type A measurement uncertainty based on repeated measurements - Worker A

Average of measured values	=PRŮMĚR()	0,115mm
Selection directional deviation	=SMODCH.VÝBĚR.S()	0,0088544mm
Average correction to 20°C	$\bar{X} \text{ korigovaný} = \bar{X} - L_{20^\circ C}$	0,115mm
u_A	$u_A = k_{UA} \cdot \frac{S}{\sqrt{n}}$	0,00280mm

Table 13. Calculation of Type A measurement uncertainty based on repeated measurements - Worker B

	Zmax	χ	u_{bi}	u_{bi}
MPE Keyence VHX	0,0038mm	1,732051	$u_{bi} = \frac{Zmax}{\chi}$	0,002193931
Temperature fluctuation 2°C	0,00000828mm	1,732051	$u_{bi} = \frac{Zmax}{\chi}$	0,000000478
Calculation of the standard combined uncertainty				
u_y	=ODMOCNINA(SUMA.ČTVERCŮ(u_A ; $u_{bivertex}$; u_{bikol}))			0,002516837
Calculation of the expanded combined uncertainty				
U	$=2 \cdot u_y$			0,006mm

Table 14. Calculation of type B measurement uncertainty and expanded combined uncertainty U - worker A [7], [8]

	Zmax	χ	u_{bi}	u_{bi}
MPE Keyence VHX	0,0038mm	1,732051	$u_{bi} = \frac{Zmax}{\chi}$	0,002193931
Temperature fluctuation 2°C	0,00000828mm	1,732051	$u_{bi} = \frac{Zmax}{\chi}$	0,000000478
Calculation of the standard combined uncertainty				
u_y	=ODMOCNINA(SUMA.ČTVERCŮ(u_A ; $u_{bivertex}$; u_{bikol}))			0,003557156
Calculation of the expanded combined uncertainty				
U	$=2 \cdot u_y$			0,008mm

Table 15. Calculation of type B measurement uncertainty and expanded combined uncertainty U - worker B [7], [8]

The measurement result of operator A with the specified expanded combined uncertainty is 0.113mm +/- 0.006mm. The measurement result of operator B with the specified expanded combined uncertainty is 0.115mm +/- 0.008mm.

7. Conclusion

This paper focuses on optimizing the clamping of HFM connectors for concentricity measurements in an accredited automotive laboratory. The research is related to the article Analysis of the effect of clamping in HMF connector measurements, where a negative effect on the measurement result due to unstable clamping of this connector was found. The experiment was performed using a Keyence VHX-5000 digital microscope with two different operators. By assessing the agreement using the EN parameter, this negative effect was demonstrated. Subsequently, the clamping optimization and subsequent recalculation were performed. This experiment was of practical benefit and helped to increase the stability of the HFM connectors. This benefit can best be demonstrated by the data obtained.

Before clamping optimization:

operator A = 0,113mm +/- 0,007mm /// operator B = 0,123mm +/- 0,011mm,

the sampling standard deviation of operator A=0,0074863mm,

the sampling standard deviation of operator B= 0,0144852mm,

u_A Operator A = 0,00237mm /// u_A Operator B = 0,00458mm,

parameter EN = 0,77.

After clamping optimization:

operator A = 0,113mm +/- 0,006mm /// operator B = 0,115mm +/- 0,008mm,

the sampling standard deviation of operator A = 0,0039001mm,

the sampling standard deviation of operator B = 0,0088544mm,

u_A operator A = 0,00123mm /// u_A operator B = 0,00280mm,

parameter EN = 0,20.

8. Acknowledgments

The article contribution has been prepared under project SGS-2022-007 - Research and Development for Innovation in Engineering Technology - Machining Technology IV.

9. References

- [1] Skrivanova, N[ikola] & Melichar, M[artin] (2019). The Comparison of Destructive and Non-Destructive Forms of Measurement in the Automotive Industry, Proceedings of the 30th DAAAM International Symposium, pp.0995-1002, B. Katalinic (Ed.), Published by DAAAM International, ISBN 978-3-90273422-8, ISSN 1726-9679, Vienna, Austria
- [2] Bicova K. Kutlwaser J., Sklenicka J.: (2016). Issue of High Precision Manufacturing Analysis in Automotive Industry, Proceedings of the 27th DAAAM International Symposium, ISBN 978-3-902734-08-2, ISSN 1726-9679, Vienna, Austria DOI: 10.2507/27th.daaam.proceedings.052
- [3] Skrivanova, N[ikola] & Melichar, M[artin] (2019). Comparing the TimeConsumption of Destructive and Non-Destructive Forms of Measurement in the Automotive Industry, Proceedings of the 30th DAAAM International Symposium, pp.1003-1007, B. Katalinic (Ed.), Published by DAAAM International, ISBN 978-3-902734-22-8, ISSN 1726-9679, Vienna, Austria
- [4] Melichar M., Kubátov D., Kutlwaše J.: (2018). The Influence of humidity on ABS plastic measurement results, Proceedings of the 29th DAAAM International Symposium, ISBN 978-3-902734-20-4, ISSN 1726-9679, Vienna, Austria DOI: 10.2507/29th.daaam.proceedings.065
- [5] Płowucha W., Kubiec W., Wojtyła M.: Possibilities of CMM Software to Support Proper Geometrical Product Verification. Procedia CIRP. Volume 43. 2016. Pages 303-308. ISSN 2212-8271. <http://dx.doi.org/10.1016/j.procir.2016.02.124>
- [6] Digitální mikroskop - VHX-5000 | KEYENCE International Belgium(Čeština). KEYENCE INTERNATIONAL (BELGIUM) NV/SA [online]. available from: <https://www.keyence.eu/cscz/products/microscope/digital-microscope/vhx-5000/models/vhx-5000/>, Accessed on: 2022-10-10
- [7] ČSN EN ISO 13005: Pokyn pro vyjádření nejistoty měření, Praha: Český normalizační institut, 2005.
- [8] MEČEK, Pavel. Nejistoty měření. 1. vydání 2008. Praha: česká společnost pro jakost,o.s., 2008. 96 s. ISBN 978-80-02-02089-9.